

## Nature of Catalytic Active Sites for Sb–V–O Mixed Metal Oxides

M. Olga Guerrero-Pérez,<sup>†,‡</sup> Taejin Kim,<sup>†</sup> Miguel A. Bañares,<sup>‡</sup> and Israel E. Wachs<sup>\*,†</sup>

*Operando Molecular Spectroscopy and Catalysis Laboratory, Department of Chemical Engineering, Lehigh University, Bethlehem, Pennsylvania 18015 and Catalytic Spectroscopy Laboratory, Instituto de Catálisis y Petroleoquímica, CSIC, C/ Marie Curie 2, E-28049 Madrid, Spain*

Received: February 27, 2008; Revised Manuscript Received: July 29, 2008

A series of bulk oxides (Sb<sub>2</sub>O<sub>3</sub>, Sb<sub>2</sub>O<sub>4</sub>, VSbO<sub>4</sub>, and V<sub>2</sub>O<sub>5</sub>) and alumina-supported oxides (Sb–O, V–O, and Sb–V–O) were synthesized by conventional methods. The resulting catalysts were characterized with XRD, BET, Raman, and CH<sub>3</sub>OH-temperature programmed surface reaction (TPSR) spectroscopy. XRD and Raman spectroscopy confirmed that the bulk oxides are present as crystalline phases and the alumina-supported oxides consisted of two-dimensional surface metal oxide species on the alumina support. In the case of alumina-supported Sb–V–O, VSbO<sub>4</sub> nanoparticles were formed from the solid-state reaction between the two oxides. CH<sub>3</sub>OH-TPSR spectroscopy was employed to determine the number (Ns) and chemical nature of active surface sites (redox and acidic) present in the formed catalysts. The bulk and alumina-supported antimonates were found to contain very few active surface redox and acid sites. In contrast, the bulk and alumina-supported vanadium oxides possess a significant number of surface redox sites with a minor amount of surface acid sites. Catalysts that possess both antimonates and vanadium oxides, however, were found to exhibit enhanced redox activity from promotion of the redox surface V<sub>x</sub> sites by the antimonates. The series of bulk and alumina-supported catalysts was examined for their performance for the selective ammoxidation of propane to acrylonitrile. Only the catalysts containing both vanadium oxide and antimonates were found active and selective for acrylonitrile formation. The enhanced performance of these catalysts is related to formation of crystalline VSbO<sub>4</sub> phases that promote the surface vanadia redox sites.

## Introduction

Vanadium–antimony mixed oxides are well known as active and selective catalysts for selective partial oxidation processes. The V–Sb–O catalysts have shown good performance for the selective oxidation of H<sub>2</sub>S to elemental sulfur,<sup>1,2</sup> oxidation of isobutene into methacrolein,<sup>3</sup> and oxidation of nitrogen organic volatile compounds;<sup>4</sup> for oxidation of methane to formaldehyde<sup>5</sup> and Sb–V–O titania-supported catalysts are used industrially for selective oxidation of *o*-xylene to phthalic anhydride.<sup>6</sup> The V–Sb–O catalysts are currently being investigated for propane selective oxidation to acrylic acid<sup>7–9</sup> and selective ammoxidation to acrylonitrile.<sup>10–13</sup> The V–Sb–O mixed oxides react to form a rutile VSbO<sub>4</sub> phase with cation vacancies.<sup>14</sup> This mixed oxide phase can take several stoichiometries near V/Sb = 1<sup>15</sup> with a general formula of Sb<sub>0.9</sub>V<sub>0.9+x</sub>O<sub>0.2-x</sub>O<sub>4</sub>.<sup>16</sup> In addition to V–Sb–O mixed oxide phases, amorphous antimony oxide,<sup>17</sup> Sb<sub>2</sub>O<sub>3</sub>, α-Sb<sub>2</sub>O<sub>4</sub>, or V<sub>2</sub>O<sub>5</sub> (Sb/V < 1) phases, may also be present. Furthermore, ion scattering spectroscopy (ISS) surface analysis of vanadium antimonite mixed oxide catalysts reveals that their surfaces are enriched with surface vanadium oxide species.<sup>18</sup>

The physicochemical properties of mixed vanadium antimony oxides have been extensively investigated in recent years;<sup>17–20</sup> however, the roles of the VSbO<sub>4</sub> phases, the dispersed surface vanadium oxide, and surface antimony oxide species during selective oxidation catalysis are not fully understood. In the present study, the nature of the catalytic active surface sites present for supported V–Sb–O catalysts are chemically probed

with CH<sub>3</sub>OH-temperature programmed reaction (TPSR) spectroscopy. The CH<sub>3</sub>OH-TPSR product distribution can show the nature of the surface active sites since redox sites yield H<sub>2</sub>CO and acid sites yield CH<sub>3</sub>OCH<sub>3</sub> as well as providing the associated surface kinetics.<sup>21</sup> Thus, methanol is a “smart” chemical probe molecule that can provide fundamental information about the number and distribution of the different types of catalytic active surface sites present in the Sb–V–O mixed oxides catalysts.<sup>22–24</sup>

## Experimental Section

**Catalyst Synthesis.** The supported Sb–V–O and Sb–O-1 catalysts were prepared by initially dissolving the required amount of antimony acetate (Aldrich) in tartaric acid (Sigma, 0.3 M).<sup>17</sup> This solution was kept stirring until all the antimony dissolved, and then NH<sub>4</sub>VO<sub>3</sub> (Sigma) and γ-Al<sub>2</sub>O<sub>3</sub> support (Girdler Südchemie) were added. Only NH<sub>4</sub>VO<sub>3</sub> was added to the alumina support to prepare V–O catalyst. In order to evaluate the effect of the antimony precursor on the dispersion of antimony oxide, a second supported Sb–O-2 catalyst was prepared from an aqueous dispersion of Sb<sub>2</sub>O<sub>3</sub> (Aldrich) to the γ-Al<sub>2</sub>O<sub>3</sub> support (Girdler Südchemie). The solution was initially dried in a rotatory evaporator at 80 °C and 0.3 atm. The resulting catalyst was further dried at 115 °C for 24 h and then calcined at 400 °C for 4 h in air. The supported catalyst compositions were maintained so that the total coverage of V + Sb, V, or Sb would correspond to the metal oxide dispersion limit or monolayer coverage on the alumina support. The dispersion limit, defined as the maximum surface loading of VO<sub>x</sub> units that remain dispersed before crystalline V<sub>2</sub>O<sub>5</sub> is formed, was determined by Raman spectroscopy to be near 9 VO<sub>x</sub> units per

\* To whom correspondence should be addressed. E-mail: ieuw0@lehigh.edu.

<sup>†</sup> Lehigh University.

<sup>‡</sup> Instituto de Catálisis y Petroleoquímica, CSIC.

square nanometer in accordance with previous characterization studies on another alumina.<sup>22</sup> The Sb/V atomic ratio was always fixed at 1.

Unsupported bulk metal oxide reference catalysts were also prepared. The bulk VSbO<sub>4</sub> reference phase was prepared by drying a solution containing equimolar concentrations of Sb and V in a rotatory evaporator at 80 °C. The Sb was added as soluble tartrate complex (Aldrich)<sup>17</sup> and V as NH<sub>4</sub>VO<sub>3</sub> (Sigma). The resulting solid was dried at 115 °C for 24 h and then calcined in air at 660 °C for 12 h and at 750 °C for 24 h. The reference  $\alpha$ -Sb<sub>2</sub>O<sub>4</sub> phase was obtained from Sb<sub>2</sub>O<sub>3</sub> after calcination in air for 30 h at 800 °C. The crystalline VSbO<sub>4</sub> and Sb<sub>2</sub>O<sub>4</sub> phases were verified with X-ray diffraction (XRD).

**XRD.** The XRD patterns were recorded on a Siemens D-501 diffractometer using Cu K $\alpha$  radiation (operation parameters of 40 kV and 22.5 mA) with registered Bragg's angles between 10° and 60°.

**BET.** Nitrogen adsorption isotherms (–196 °C) were recorded on an automated Micromeritics ASAP-2000 apparatus. Prior to the adsorption experiments samples were outgassed at 413 K for 2 h. The BET surface area was computed from the adsorption isotherms ( $0.05 < P/P_0 < 0.27$ ) with a value of 0.164 nm<sup>2</sup> for the cross-section of the adsorbed N<sub>2</sub> molecule at –196 °C.

**Raman.** Raman spectra were obtained with a single monochromator system (Renishaw 1000) equipped with a cooled CCD detector (–73 °C) and a holographic super-Notch filter. The catalysts samples were excited with 514 nm (visible green line). The Raman spectra of the dehydrated catalysts were obtained after dehydration at ~120 °C under flowing dry air in a hot stage (Linkam TS-1500). The Raman spectra of the hydrated catalyst samples were obtained at room temperature after exposure to a stream of humid synthetic air.

**TPSR.** The surface chemistry and reactivity of the supported vanadium oxide catalysts were chemically probed with CH<sub>3</sub>OH-TPSR spectroscopy (Altamira AMI-200) equipped with an online quadrupole mass spectrometer (Dycor Dymaxion DME200MS). The catalysts were pretreated at 400 °C in flowing 10% O<sub>2</sub>/He (Airgas, Ultra Zero grade Air, 30 mL/min) for 40 min to remove moisture and any possible oxidizable surface residues. The catalysts were subsequently cooled in the oxidizing environment to 110 °C and then switched to flowing He (Airgas, Ultra High Purity, 30 mL/min) and further cooled to 100 °C. The methanol was chemisorbed at 100 °C from a CH<sub>3</sub>OH/He flowing mixture (Airgas, 2000 ppm CH<sub>3</sub>OH, 30 mL/min) for 30 min. Previous work demonstrated that methanol adsorption at 100 °C minimizes formation of physically adsorbed methanol on the samples since physically adsorbed CH<sub>3</sub>OH desorbs below this temperature from oxide surfaces.<sup>22–25</sup> After adsorption of CH<sub>3</sub>OH on the catalysts, the samples were purged for 1 h in flowing He to remove any residual physically adsorbed methanol and the sample temperature was then increased in the flowing He at a heating rate of 10 °C/min. The reaction products desorbing from the catalysts were monitored with the online mass spectrometer (MS). The *m/e* values of CH<sub>3</sub>OH (*m/e* = 31), HCHO (*m/e* = 30), CH<sub>3</sub>OCH<sub>3</sub> (*m/e* = 45), CO (*m/e* = 28), and CO<sub>2</sub> (*m/e* = 44) were employed to detect the different desorption products.

**Propane Ammoxidation.** The steady-state propane ammoxidation catalytic measurements were performed with a conventional quartz microreactor (ED = 9 mm, ID = 7.8 mm, length = 290 mm) coupled to an online gas chromatograph (Varian CP-3800) equipped with both flame ionization and thermal conductivity detectors. The GC columns consisted of molecular

**TABLE 1: BET Area Values of Supported V–Sb–O Catalysts**

	BET surface area (m <sup>2</sup> /g)
Al <sub>2</sub> O <sub>3</sub>	160
Sb–V–O	139
V–O	130
Sb–O-1	122
Sb–O-2	105

sieves and a Porapak Q, respectively. The accuracy of the analytical measurements was checked for each test by verification that the carbon balance was within the cumulative mean error of  $\pm 10\%$  based on the propane converted. The catalytic reaction tests employed 0.2 g of sample with particle dimensions in the 0.25–0.125 mm range. The catalysts were located between two quartz wool beds and pretreated in a volumetric mixture of 30% of O<sub>2</sub> in He at 200 °C for 1 h. The axial temperature profile, which was always isothermal, was monitored by a sliding thermocouple inside a tube inserted into the catalyst bed. The reactant gas composition consisted of 25% O<sub>2</sub>, 9.8% propane, 8.6% ammonia, and balance helium. The total flow rate was maintained at 20 cc/min and corresponded to a gas-space velocity (GHSV) of about 3000 h<sup>–1</sup>. The quantities of catalyst and total flow were determined in our previous work in order to avoid internal and external diffusion limitations.<sup>26</sup> The yield and selectivity of the reaction products were determined on the basis of the moles of propane in the feed and products as well as considering the number of carbon atoms in each molecule.

## Results

**BET.** The BET surface area values of the supported catalysts are listed in the Table 1. The BET values for the supported Sb–V–O, V–O, Sb–O-1, and Sb–O-2 catalyst samples are all in excess of 100 m<sup>2</sup>/g because they are dominated by the high surface area of the alumina support (160 m<sup>2</sup>/g). The decrease in BET values for the Al<sub>2</sub>O<sub>3</sub>-supported catalysts is a consequence of the added mass of the supported metal oxide phase. In contrast, the BET surface area values of the reference unsupported VSbO<sub>4</sub> and Sb<sub>2</sub>O<sub>4</sub> bulk phases are below 5 m<sup>2</sup>/g and cannot be determined precisely by N<sub>2</sub> physisorption.

**In Situ Raman Spectroscopy.** The ambient Raman spectra of the unsupported, bulk crystalline Sb<sub>2</sub>O<sub>3</sub>, Sb<sub>2</sub>O<sub>4</sub>, V<sub>2</sub>O<sub>5</sub>, and VSbO<sub>4</sub> phases, confirmed with XRD, are presented in Figure 1. The unsupported, bulk reference samples Sb<sub>2</sub>O<sub>3</sub> (190, 255, 372, 451, 716 cm<sup>–1</sup>), Sb<sub>2</sub>O<sub>4</sub> (190, 261, 399, 459 cm<sup>–1</sup>), and V<sub>2</sub>O<sub>5</sub> (143, 283, 302, 405, 480, 526, 698, 994 cm<sup>–1</sup>) give rise to multiple sharp Raman bands. The unsupported, bulk VSbO<sub>4</sub> reference sample, however, exhibits a broad Raman band between 700 and 900 cm<sup>–1</sup>.<sup>11</sup>

The in situ Raman spectra of the dehydrated alumina-supported Sb–V–O, V–O, Sb–O-1, and Sb–O-2 catalysts are presented in Figure 2. The supported Sb–O-1 catalyst, prepared from Sb–acetate and addition of tartaric acid, contains broad and weak Raman bands at 780, 600, 468, and 210 cm<sup>–1</sup>, which do not correspond to the Raman bands of crystalline Sb<sub>2</sub>O<sub>3</sub> and Sb<sub>2</sub>O<sub>4</sub>. These Raman bands have previously been assigned to an amorphous antimony oxide phase interacting with the Al<sub>2</sub>O<sub>3</sub> support.<sup>17</sup> The dehydrated supported Sb–O-2 catalyst, prepared with bulk Sb<sub>2</sub>O<sub>3</sub> in the absence of tartaric acid, also exhibits the broad bands corresponding to an amorphous antimony oxide phase on the Al<sub>2</sub>O<sub>3</sub> support as well as a sharp band at ~198 cm<sup>–1</sup> characteristic of crystalline Sb<sub>2</sub>O<sub>4</sub>. The Raman spectra of the dehydrated supported Sb–V–O and V–O catalysts contain

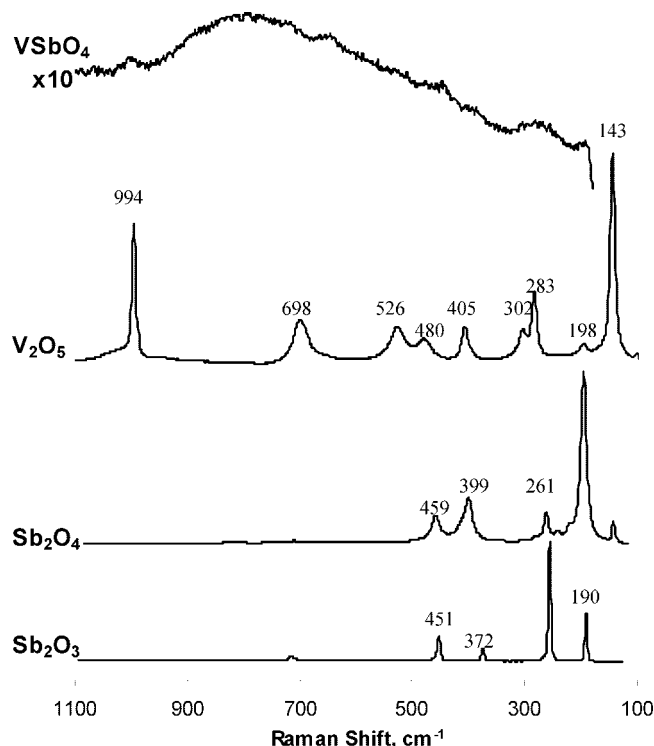


**Figure 1.** Raman spectra of unsupported bulk  $\text{Sb}_2\text{O}_4$ ,  $\text{Sb}_2\text{O}_3$ ,  $\text{V}_2\text{O}_5$ , and  $\text{VSbO}_4$  mixed oxides.

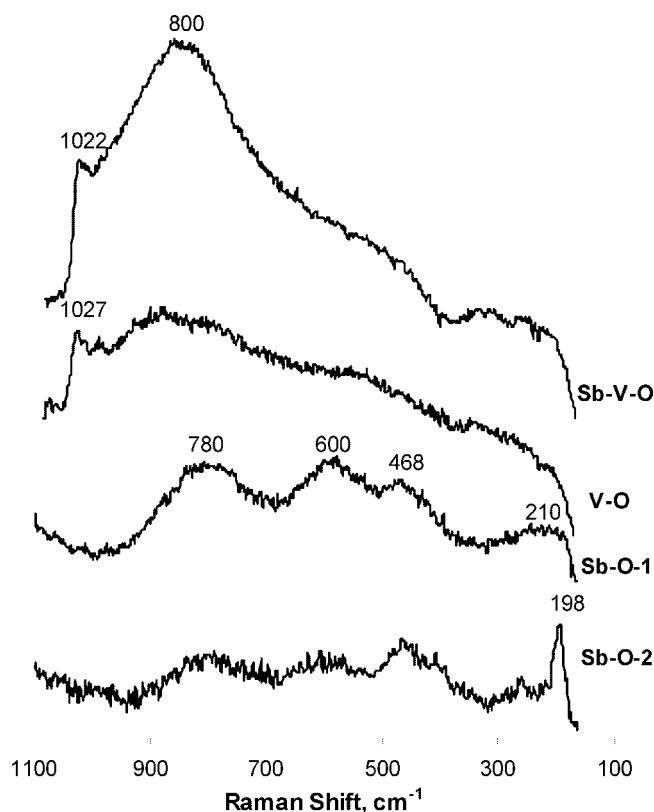


**Figure 2.** In situ Raman spectra of dehydrated alumina-supported V-Sb-O catalysts.

sharp bands at  $\sim 1022$  and  $\sim 1027$   $\text{cm}^{-1}$ , respectively, that are very sensitive to hydration. The sensitivity of the bands at 1022 and 1027  $\text{cm}^{-1}$  to hydration/dehydration is characteristic of dispersed surface  $\text{VO}_x$  species on the alumina support.<sup>27</sup> The dehydrated supported Sb-V-O catalyst also possesses a broad Raman band at  $\sim 800$   $\text{cm}^{-1}$  that has previously been ascribed

to two Raman bands associated with alumina-supported crystalline  $\text{VSbO}_4$  mixed oxide nanoparticles (NPs).<sup>11</sup> Surface  $\text{SbO}_x$  species may also be present for the supported Sb-V-O catalyst, but the bands from the surface  $\text{SbO}_x$  species overlap those of the  $\text{SbVO}_4$  NPs, and their presence cannot be confirmed from Raman spectroscopy.

**$\text{CH}_3\text{OH}$ -TPSR.**  $\text{CH}_3\text{OH}$ -TPSR spectroscopy studies were undertaken to chemically probe the surface chemistry of the unsupported, bulk, and alumina-supported Sb-V-O catalysts. The bulk  $\text{Sb}_2\text{O}_4$  reference oxide was found to be inactive for methanol surface chemistry during  $\text{CH}_3\text{OH}$ -TPSR even when significant amounts of sample were employed to compensate for its low BET surface area and did not give rise to any reaction products (not shown for brevity). This is in agreement with previous studies that found the bulk antimony oxide to have extremely low activity surface redox sites ( $T_p = 375$  °C).<sup>28</sup> Consequently, the  $\text{Sb}_2\text{O}_4$  bulk oxide, and presumably  $\text{Sb}_2\text{O}_3$ , does not possess very active catalytic sites. In contrast, the low BET surface area bulk  $\text{V}_2\text{O}_5$  and  $\text{VSbO}_4$  samples do possess active surface sites. The  $\text{CH}_3\text{OH}$ -TPSR for bulk  $\text{V}_2\text{O}_5$  was previously investigated<sup>23</sup> and found to exclusively give rise to  $\text{H}_2\text{CO}$  ( $T_p = 188$  °C) from surface  $\text{V}^{5+}$  redox sites. The  $\text{CH}_3\text{OH}$ -TPSR spectra for the bulk  $\text{VSbO}_4$  mixed oxide are shown in Figure 3. Bulk  $\text{VSbO}_4$  gives rise to significant production of  $\text{HCHO}$  ( $T_p \approx 150$  °C) from surface redox sites. The very low  $T_p$  of  $\sim 150$  °C indicates that the surface redox sites for bulk  $\text{VSbO}_4$  are extremely active and the vanadia sites are being promoted by antimony.<sup>23,24</sup> The  $\text{CH}_3\text{OH}$ -TPSR spectra from the native alumina support are shown in Figure 3. The pure  $\text{Al}_2\text{O}_3$  support only gives rise to DME from surface Lewis acid ( $T_p \approx 196$  °C) and does not possess any redox surface sites.

The  $\text{CH}_3\text{OH}$ -TPSR spectra for the alumina-supported V-O, Sb-O-1, Sb-O-2, and Sb-V-O catalysts are also contained in Figure 3. The supported V-O catalyst consists of a monolayer of surface  $\text{VO}_x$  species and mostly yields  $\text{H}_2\text{CO}$  ( $T_p \approx 197$  °C) with some minor formation of DME ( $T_p \approx 212$  °C). The extensive suppression of the surface acid sites for the supported V-O sample reflects the two-dimensional monolayer of the surface  $\text{VO}_x$  species on the  $\text{Al}_2\text{O}_3$  support. The supported Sb-O-1 catalyst, which contains an amorphous  $\text{SbO}_x$  phase on alumina (see Figure 2), also suppresses  $\text{HCHO}$  production and yields modest amounts of DME ( $T_p \approx 222$  °C), reflecting the high dispersion of this amorphous layer over the acidic alumina support. The supported Sb-O-2 catalyst, which contains both an amorphous phase and crystalline  $\text{Sb}_2\text{O}_4$  NPs (see Figure 2), however, forms significant amounts of DME ( $T_p \approx 194$  °C) and traces of  $\text{H}_2\text{CO}$  ( $T_p \approx 197$  °C), reflecting the poor dispersion of  $\text{SbO}_x$  on  $\text{Al}_2\text{O}_3$  starting from the bulk  $\text{Sb}_2\text{O}_3$  precursor. The lack of significant  $\text{HCHO}$  formation for both Sb-O-1 and Sb-O-2 catalysts ( $T_p \approx 197$  and 221 °C, respectively) also reflects on the low redox characteristics as well as overall reactivity of the supported  $\text{SbO}_x$  phase on the  $\text{Al}_2\text{O}_3$  support. The supported Sb-V-O sample gives rise to significant  $\text{HCHO}$  production (very broad peak with  $T_p \approx 197$  °C) from surface redox sites. The broad  $\text{HCHO}$ -TPSR peak from the alumina-supported Sb-V-O sample almost looks like a composite of the TPSR spectra from bulk  $\text{VSbO}_4$  and alumina-supported V-O catalysts. The almost complete absence of DME formation from the surface acid sites of the alumina support reflects that Sb-V-O phase is well dispersed on the  $\text{Al}_2\text{O}_3$  support and suggests that both surface  $\text{VO}_x$  and  $\text{SbO}_x$  species are almost completely covering the alumina support.

The first-order kinetic parameters for  $\text{H}_2\text{CO}$  and DME formation are given in Table 2 as well as the corresponding  $T_p$

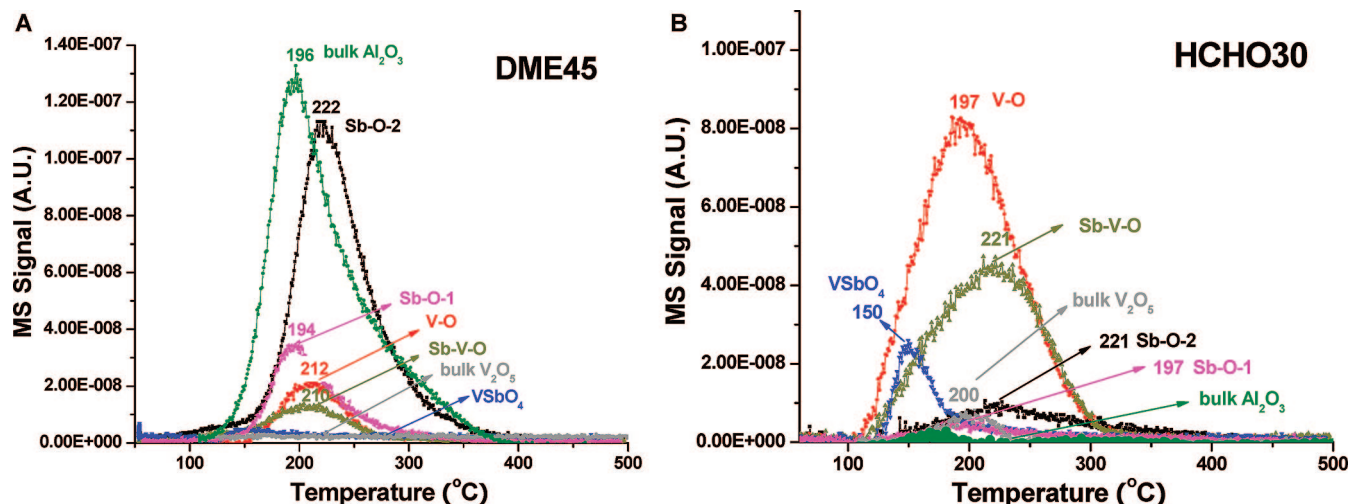


**Figure 3.** CH<sub>3</sub>OH temperature-programmed surface reaction (TPSR) spectra from Sb–O–1, Sb–O–2, V–O, Sb–V–O, V<sub>2</sub>O<sub>5</sub>, and VSbO<sub>4</sub> samples: (A) DME45 and (B) HCHO30. He flow rate = 30 cm<sup>3</sup>/min. Temperature ramping rate = 10 °C/min. The amount of sample was 500 mg for VSbO<sub>4</sub> and 100 mg for the rest of samples.

**TABLE 2: Kinetic Parameters Obtained From the CH<sub>3</sub>OH-TPSR Experiments with a He Flow Rate = 30 cm<sup>3</sup>/min and a Heating Rate of 10 °C/min<sup>a</sup>**

samples	peak temperature (°C)		$E_a$ (kcal/mol)		$k_{rds}$ (s <sup>-1</sup> )		total number of redox sites (sites/g)
	DME	HCHO	DME	HCHO	DME	HCHO	
Al <sub>2</sub> O <sub>3</sub>	196		32.0		0.12		
Sb–O–1	194	197	31.9	32.1	0.14	0.12	8.6E+19
Sb–O–2	222	221	33.8	33.8	0.02	0.02	1.8E+20
V–O	212	197	33.1	32.1	0.04	0.12	1.2E+21
Sb–V–O	210	221	33.0	33.8	0.05	0.02	7.3E+20
VSbO <sub>4</sub>		150		28.8		3.12	4.0E+19
V <sub>2</sub> O <sub>5</sub>		200		32.3		0.09	5.1E+18 <sup>a</sup>

<sup>a</sup> Data from ref 28.

values. The supported metal oxide catalysts behave very similarly and possess  $E_a$  values of 32–34 kcal/mol and Arrhenius rate constants of 0.02–0.12 s<sup>-1</sup> for HCHO formation and 0.02–0.14 s<sup>-1</sup> DME formation at a reference temperature of 230 °C. In contrast, the unsupported VSbO<sub>4</sub> catalyst exhibits a lower  $E_a$  of ~29 kcal/mol and a first-order rate constant of 3.12 s<sup>-1</sup> for H<sub>2</sub>CO formation at a reference temperature of 230 °C. Thus, the bulk VSbO<sub>4</sub> catalyst possesses highly active catalytic redox sites.

The number of redox sites ( $N_s$ ) chemically probed by CH<sub>3</sub>OH during the TPSR experiment are also listed in Table 2. For the most part, DME production from the alumina-supported catalysts is assumed to be associated with the surface acidic sites of the alumina support. It is clear that similar to the bulk Sb<sub>2</sub>O<sub>3</sub> and Sb<sub>2</sub>O<sub>4</sub> phases, the alumina-supported SbO<sub>x</sub> phases in Sb–O–1 and Sb–O–2 are not very active and possess few redox sites. It appears that the dispersed SbO<sub>x</sub> layer on Al<sub>2</sub>O<sub>3</sub> (Sb–O–1) has somewhat less redox sites than the Sb–O–2 catalyst containing both crystalline Sb<sub>2</sub>O<sub>4</sub> and the dispersed SbO<sub>x</sub> phase. In contrast to the alumina-supported Sb–O catalysts, the alumina-supported V–O and Sb–V–O catalysts contain a large amount of redox sites that is associated with the presence of the vanadium oxide component. Bulk VSbO<sub>4</sub> and V<sub>2</sub>O<sub>5</sub> also exhibit significant amounts of redox sites without the copresence of acid sites, but the number of sites/gram is low because of the low BET surface areas of these bulk metal oxides.

**Propane Ammoxidation.** The steady-state propane ammoxidation catalytic results at 440 °C are presented in Figure 4, and the corresponding activity and TOF values are given in Table 3. Both the pure Al<sub>2</sub>O<sub>3</sub> support and the supported Sb–O–1 and

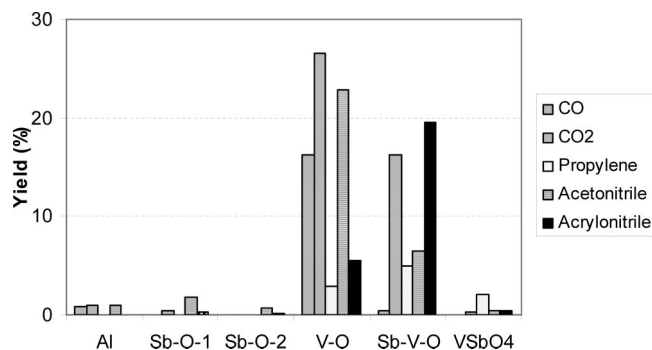


**Figure 4.** Propane ammoxidation yield to principal reaction products. Reaction conditions: temperature, 420 °C; total flow, 20 mL/min; feed composition (% volume), C<sub>3</sub>H<sub>8</sub>/O<sub>2</sub>/NH<sub>3</sub> (9.8/25/8.6); 200 mg of catalyst.

Sb–O–2 catalysts are highly inefficient for acrylonitrile formation as found for the unsupported bulk  $\alpha$ -Sb<sub>2</sub>O<sub>4</sub> oxide phase.<sup>29</sup> This is a consequence of the absence of redox sites for Al<sub>2</sub>O<sub>3</sub> and the low redox properties of the alumina-supported Sb–O–1 and Sb–O–2 catalysts. The presence of vanadium oxide is critical for introduction of redox sites. The surface vanadium oxide species on the alumina-supported V–O do form acrylonitrile, but the very active catalyst mainly yields decomposition products (CO, CO<sub>2</sub>, and acetonitrile). Nevertheless, the acrylonitrile TOF for alumina-supported V–O is ~20 times greater than that for the alumina-supported antimony oxide catalysts. Bulk V<sub>2</sub>O<sub>5</sub>, however, is also selective to total oxidation and decomposition products (CO, CO<sub>2</sub>, and acetonitrile) as well as catalyzing the unselective conversion of NH<sub>3</sub> to N<sub>2</sub>.<sup>30,31</sup> Only

**TABLE 3: Acrylonitrile Formation Rate and TOF Values during Propane Ammoxidation Reaction<sup>a</sup>**

samples	activity (mmol acrylonitrile/g·s)	TOF <sup>b</sup> (s <sup>-1</sup> )	TOF <sup>c</sup> (s <sup>-1</sup> )
Sb–O-1	0.009	0.12	0.01
Sb–O-2	0.003	0.02	0.00
V–O	0.200	0.20	0.21
Sb–V–O	0.715	1.18	0.14
VSbO <sub>4</sub>	0.016	0.10	

<sup>a</sup> The number of surface redox sites is determined by methanol chemisorption obtained from the CH<sub>3</sub>OH-TPSR experiments with He flow rate = 30 cm<sup>3</sup>/min and a heating rate of 10 °C/min. Propane ammoxidation reaction conditions: temperature: 420°C, total flow, 20 mL/min; feed composition (% volume), C<sub>3</sub>H<sub>8</sub>/O<sub>2</sub>/NH<sub>3</sub> (9.8/25/8.6), 200 mg of catalyst. <sup>b</sup> Considering redox active sites. <sup>c</sup> Considering total Sb + V atoms supported on the alumina support.

for alumina-supported Sb–V–O, where both SbO<sub>x</sub> and VO<sub>x</sub> are simultaneously present, does the system become selective to acrylonitrile formation and a further increase in the acrylonitrile TOF is obtained (factor of ~3–5). The unsupported bulk VSbO<sub>4</sub> phase is not as selective toward acrylonitrile formation as the supported V–Sb–O catalyst, and its main reaction product is propylene. The large amount of propylene reflects the low propane conversion achieved with this low BET surface area catalyst. On the basis of the number of redox sites determined with CH<sub>3</sub>OH-TPSR, the acrylonitrile TOF value for bulk VSbO<sub>4</sub> is greater than that for alumina-supported Sb–O-1 and Sb–O-2 and comparable to that for the alumina-supported V–O monolayer. If all the propylene were to be converted to acrylonitrile at higher conversions, then the apparent acrylonitrile TOF would be increased by a factor of ~5 and comparable to that of the alumina-supported Sb–V–O catalyst.

## Discussion

**SbO<sub>x</sub> Sites.** Bulk VSbO<sub>4</sub> and Sb<sub>2</sub>O<sub>3</sub> are resistant toward reduction,<sup>18</sup> and their CH<sub>3</sub>OH-TPSR spectra exhibit HCHO *T<sub>p</sub>* of ~375 °C, which reflects their low redox character.<sup>28</sup> The methanol oxidation chemical probe reaction also reveals that surface acid sites are not present for the bulk antimony oxides.<sup>28</sup> The alumina-supported Sb–O-1 catalyst contains almost no surface acidic sites, which is consistent with a layer of amorphous Sb oxide species covering the Al<sub>2</sub>O<sub>3</sub> support. In contrast, the alumina-supported Sb–O-2 catalyst possesses crystalline Sb<sub>2</sub>O<sub>4</sub> nanoparticles at comparable Sb loading. Consequently, exposed alumina sites are present that are responsible for the acidic surface character of alumina-supported Sb–O-2 sample. The number of surface redox sites present for alumina-supported Sb–O-1 and Sb–O-2 catalysts is extremely low and seems to follow the bulk antimony oxide characteristics (Table 3). Crystalline Sb<sub>2</sub>O<sub>4</sub> NPs possess even less redox character than the surface Sb<sub>x</sub> species that are coordinated to the Al<sub>2</sub>O<sub>3</sub> support.

**VO<sub>x</sub> Sites.** The characterization studies demonstrated that the supported V–O catalyst consists of approximately a monolayer of surface VO<sub>x</sub> sites on the Al<sub>2</sub>O<sub>3</sub> support that primarily possess redox character. This property follows the known features of bulk V<sub>2</sub>O<sub>5</sub> crystallites.<sup>28,32</sup> The redox surface VO<sub>x</sub> sites can form propylene and acrolein partial oxidation products, but they also form significant amounts of decomposition or combustion products. The similar *T<sub>p</sub>* for H<sub>2</sub>CO near 190 °C for both bulk V<sub>2</sub>O<sub>5</sub> and alumina-supported VO<sub>x</sub> suggests that primarily surface V<sup>5+</sup> redox sites are present. The large amount of redox sites (Table 3) is responsible of the high activity observed for the alumina-supported V–O sample (Figure 4) during the propane

ammoxidation reaction. The supported V–O catalyst, however, is not selective to partial oxidation products since it mainly yields combustion (CO and CO<sub>2</sub>) and decomposition (acetonitrile) reaction products (Figure 4). Consequently, the acrylonitrile TOF values for alumina-supported VO<sub>x</sub> are modest. It is possible that the minor amounts of surface acid sites associated with the surface VO<sub>x</sub> monolayer may also be contributing to the lower acrylonitrile TOF.<sup>22,31,32</sup>

**VSbO<sub>4</sub> Sites.** Bulk VSbO<sub>4</sub> (rutile) essentially exhibits highly reactive redox sites (see Figure 3) with *T<sub>p</sub>* ≈ 150 °C and a *k<sub>rds,HCHO</sub>* value that is 10<sup>1</sup>–10<sup>2</sup> greater than the other catalyst samples (Table 2). The alumina-supported Sb–V–O catalyst contains surface VO<sub>x</sub> species, surface SbO<sub>x</sub> species, and crystalline VSbO<sub>4</sub> NPs. The surface SbO<sub>x</sub> species are not active for redox reactions, and only the surface VO<sub>x</sub> and VSbO<sub>4</sub> NPs possess significant redox character (see Figure 3). The enhanced activity and selectivity of the supported Sb–V–O catalyst toward acrylonitrile formation relative to the alumina-supported V–O monolayer catalyst is, thus, primarily related to the VSbO<sub>4</sub> NPs. Furthermore, as mentioned earlier, the propane ammoxidation TOF over the unsupported VSbO<sub>4</sub> is comparable to that for the alumina-supported Sb–V–O catalyst. Thus, the crystalline VSbO<sub>4</sub> phase is responsible for the enhanced catalytic activity and selectivity of alumina-supported Sb–V–O catalysts.

Although SbO<sub>x</sub> is not catalytically active for redox reactions, it seems to moderate the activity and selectivity of vanadium oxide. The surface VO<sub>x</sub> species present on crystalline VSbO<sub>4</sub> particles are very active redox sites (see Figure 3). This suggests that surface VO<sub>x</sub> sites on VSbO<sub>4</sub> crystallites are activated by the properties of the underlying “VSbO<sub>4</sub>” support. The surface SbO<sub>x</sub> species appear to moderate the activity of the surface VO<sub>x</sub> species on Al<sub>2</sub>O<sub>3</sub> so that they are not as active for combustion and decomposition of the C<sub>3</sub> compounds. These characteristics of antimony oxide reveal the promotional effect that antimony oxide has upon vanadium oxide-containing catalysts.

## Conclusions

Both bulk and supported antimony oxides possess very few surface redox sites and essentially no surface acid sites. Consequently, they are not active redox sites for propane ammoxidation to acrylonitrile. In contrast, bulk and supported vanadium oxides contain many surface redox sites and few surface acid sites. The high activity of the vanadium oxide surface sites, however, tends to also result in combustion and decomposition products. The interaction between antimony oxides and vanadium oxides, however, leads to formation of redox sites with enhanced catalytic activity. Consequently, catalytic materials containing bulk VSbO<sub>4</sub> or supported Sb–V–O phases exhibit enhanced redox activity for selective oxidation reactions such as propane ammoxidation to acrylonitrile.

**Acknowledgment.** M.O.G.-P. thanks the Operando Molecular Spectroscopy & Catalysis Laboratory at Lehigh University for financial support during her stay. Support from the Department of Energy, Division of Basic Energy Sciences (grant no. DE-FG 02-93 ER 14350), and the Spanish Ministry of Education and Science (project no. CTQ2005-02802/PPQ) for this work is gratefully acknowledged.

## References and Notes

- (1) Kim, B. G.; Park, D. W.; Kim, I.; Woo, H. C. *Catal. Today* **2003**, *87*, 11.
- (2) Li, K. T.; Wu, K. S. *Ind. Eng. Chem. Res.* **2001**, *40*, 1052.
- (3) Shishido, T.; Inoue, A.; Konishi, T.; Matsuura, I.; Takehira, K. *Catal. Lett.* **2000**, *68*, 215.

- (4) Guerrero-Pérez, M. O.; Janas, J.; Machej, T.; Haber, J.; Lewandowska, A. E.; Fierro, J. L. G.; Bañares, M. A. *Appl. Catal. B* **2007**, *71*, 85.
- (5) Sang, H.; Sang, J.; Sun, K.; Feng, Z.; Ying, P.; Li, C. *Catal. Lett.* **2006**, *106*, 89.
- (6) Saleh, R. Y.; Wachs, I. E. Carboxylic Anhydride Process, *U.S. Patent 4,855,457*, Aug 8, 1989.
- (7) Blasco, T.; Botella, P.; Concepción, P.; López-Nieto, J. M.; Martínez-Arias, A.; Prieto, C. *J. Catal.* **2004**, *228*, 362.
- (8) Al-Saedi, J. M.; Gulians, V. V.; Guerrero-Pérez, M. O.; Bañares, M. A. *J. Catal.* **2003**, *215*, 108.
- (9) Gulians, V. V.; Bhandari, R.; Al-Saedi, J. N.; Vasudevan, V. K.; Soman, R.; Guerrero-Pérez, O.; Bañares, M. A. *Appl. Catal., A* **2004**, *274*, 123.
- (10) Grasselli, R. K. *Top. Catal.* **2003**, *23*, 5.
- (11) Guerrero-Pérez, M. O.; Fierro, J. L. G.; Vicente, M. A.; Bañares, M. A. *J. Catal.* **2002**, *206*, 339.
- (12) Guerrero-Pérez, M. O.; Al-Saedi, J. N.; Gulians, V. V.; Bañares, M. A. *Appl. Catal., A* **2004**, *260*, 93.
- (13) Guerrero-Pérez, M. O.; Martínez-Huerta, M. V.; Fierro, J. L. G.; Bañares, M. A. *Appl. Catal., A* **2006**, *298*, 110.
- (14) Berry, F. J.; Brett, M. E. *Inorg. Chim. Acta* **1983**, *7*, L205.
- (15) Brazdil, J. F.; Toft, M. A.; Barket, J. P.; Teller, R. G.; Cyngier, R. *Chem. Matter* **1998**, *10*, 4100.
- (16) Landa-Cánovas, A.; Nilsson, H.; Hansen, S.; Stal, K.; Andersson, A. *J. Solid State Chem.* **1995**, *116*, 369.
- (17) Guerrero-Pérez, M. O.; Fierro, J. L. G.; Bañares, M. A. *Top. Catal.* **2006**, *41*, 43.
- (18) Zanthoff, H. W.; Grünert, W.; Buchholz, S.; Heber, M.; Silvano, L.; Wagner, F. E.; Wolf, G. U. *J. Mol. Catal. A* **2000**, *162*, 443.
- (19) Stievano, L.; Wagner, F. E.; Zanthoff, H. W.; Calogero, S. *Hyperfine Interact.* **2002**, *141/142*, 397.
- (20) Guerrero-Pérez, M. O.; Bañares, M. A. *J. Phys. Chem. C* **2007**, *111*, 1315.
- (21) Tatibouet, J. M. *Appl. Catal., A* **1997**, *148*, 213.
- (22) Briand, L. E.; Farneth, W. E.; Wachs, I. E. *Catal. Today* **2000**, *62*, 219.
- (23) Wang, X.; Wachs, I. E. *Catal. Today* **2004**, *96*, 211.
- (24) Wachs, I. E.; Jehng, J.-M.; Ueda, W. *J. Phys. Chem. B* **2005**, *109*, 2275.
- (25) Wachs, I. E.; Briand, L. E.; Jehng, J.-M.; Burcham, L.; Gao, X. *Catal. Today* **2000**, *57*, 323.
- (26) Guerrero-Pérez, M. O.; Peña, M. A.; Fierro, J. L. G.; Bañares, M. A. *Ind. Eng. Chem. Res.* **2006**, *45*, 4537.
- (27) Bañares, M. A.; Wachs, I. E. *J. Raman Spectrosc.* **2002**, *33*, 259.
- (28) Badlani, M.; Wachs, I. E. *Catal. Lett.* **2001**, *75*, 137.
- (29) Centi, G.; Mazzoli, P. *Catal. Today* **1996**, *28*, 351.
- (30) Andersson, S. L. T.; Andersson, C. G.; Grasselli, R. K.; Sanati, M.; Trifiro, F. *Stud. Surf. Sci. Catal.* **1993**, *75*, 691.
- (31) Andersson, S. L. T.; Andersson, C. G.; Grasselli, R. K.; Sanati, M.; Trifiro, F. *Appl. Catal., A* **1994**, *113*, 43.
- (32) Jih-Mirn Jehng, J. M.; Ueda, W.; Wachs, I. E. *J. Phys. Chem. B* **2005**, *109*, 2275.

JP801701M